Effects of NAD^+ Binding on the Luminescence of Tryptophans 84 and 310 of Glyceraldehyde-3-phosphate Dehydrogenase from *Bacillus stearothermophilus*†

Edi Gabellieri,‡ Sophie Rahuel-Clermont,§ Guy Branlant,§ and Giovanni B. Strambini*,‡

Istituto di Biofisica—CNR, Via S. Lorenzo, 26, 56127 Pisa, Italy, and Laboratoire d'Enzymologie et de Génie Génétique, Université Henri Poincaré, Nancy I, URA CNRS 457, B.P. 239, 54506 Vandoeuvre-Lès-Nancy Cédex, France

Received January 30, 1996; Revised Manuscript Received July 18, 1996⊗

ABSTRACT: The individual fluorescence and phosphorescence properties of W84 and W310 in *Bacillus stearothermophilus* glyceraldehyde-3-phosphate dehydrogenase were identified through the construction of a single tryptophan mutant (W84F) and by comparison of the emission between mutant and wild-type enzymes. The results show that the luminescence of W310 is red-shifted and substantially quenched relative to that of W84. It displays an average subnanosecond fluorescence lifetime (τ_F) and a very short, 50 μs, room-temperature phosphorescence (RTP) lifetime (τ_P). The perturbation of W310 luminescence is believed to arise from a stacking interaction with Y283. In contrast, W84 exhibits a fluorescence lifetime τ_F of several nanoseconds and a long-lived phosphorescence lifetime τ_P, typical of buried, unperturbed Trp residues. NAD^+ binding to the tetrameric enzyme causes a 55% reduction of W310 fluorescence intensity together with a nearly complete quenching of its low-temperature phosphorescence. W84, which is located far from the nicotinamide moiety of NAD^+, is much less affected by the binding of the coenzyme; the reduction in fluorescence intensity is 35%, and its phosphorescence intensity is unchanged. Another consequence of NAD^+ binding is a significant decrease of the RTP lifetime τ_P of W84, manifesting thereby a conformational change in the region of the coenzyme-binding domain. However, no change is observed in the RTP lifetime τ_P of W310 located in the catalytic domain. These findings and those obtained at partial coenzyme saturation support the conclusions derived from high-resolution crystallographic structures [Skarzynski, T., & Wonacott, A. J., (1988) *J. Mol. Biol. 203*, 1097−1118] that the NAD^+-induced conformational change is sequential and that subtle rearrangement in the structure of unligated subunits might be responsible for the negative cooperative behavior of NAD^+ binding.

Two major models have been proposed to explain negative cooperative ligand binding to an oligomeric protein. In the preexisting asymmetry model (Malhotra & Bernhardt, 1968; Seydoux et al., 1974), a symmetric and an asymmetric quaternary conformation of the protein are in equilibrium in solution. Negative cooperativity is a consequence of ligand binding to the asymmetric state, which possesses two different classes of binding sites arising from structural asymmetry. Alternatively, the induced-fit model introduced by Koshland et al. (1966) allows intermediate asymmetric conformations between symmetric unligated and fully ligated states. Ligand binding sequentially induces a conformational change of the bound subunit, giving rise to structural rearrangements in the unligated sites of the oligomer and resulting in the negative cooperative effect observed.

Many of the concepts about negative cooperativity of proteins have been derived from studies on phosphorylating glyceraldehyde-3-phosphate dehydrogenase (GAPDH).[1] GAPDH is a homotetrameric enzyme whose sequence has been determined from several species and appears to be highly conserved. Furthermore, on the basis of the ease with which enzymes from phylogenetically distant sources are able to form hybrid tetramers, a high degree of conservation is predicted also for the tertiary and quaternary structure (Harris & Waters, 1976). Indeed, the three-dimensional structures of holo-GAPDH of *Bacillus stearothermophilus* (Biesecker et al., 1977; Skarzynski et al., 1987), lobster (Moras et al., 1975), and *Escherichia coli* (Duee et al., 1996) have been determined by radiocrystallography and show high similarity. The structure of the GAPDH monomer comprises a catalytic domain and a coenzyme-binding domain which shares the structural features typical of NAD dehydrogenases.

GAPDH isolated either from muscle (Conway & Koshland, 1968; Trentham, 1968; Seydoux et al., 1973), *B. stearothermophilus* (Allen & Harris, 1975), or *E. coli* (Branlant & Branlant, 1985; Corbier et al., 1990) exhibits negative cooperativity in binding the coenzyme NAD^+. On the basis of the X-ray crystallographic data, it is difficult to discriminate between the preexisting asymmetry model and the induced-fit model. The interpretation of crystallographic data obtained on the lobster enzyme by Moras et al. (1975) showed possible asymmetry between the subunits in which the active centers are closely related across the R axis and thus supported the first model. In contrast, the crystallographic data obtained by Wonacott's group on *B. stearo-*

† This work was supported by the Centre National de la Recherche Scientifique, the Université Henri Poincaré, Nancy I, and the Consiglio Nazionale delle Ricerche.

* To whom correspondence should be addressed.
‡ Istituto di Biofisica—CNR.
§ Université Henri Poincaré, Nancy I.

⊗ Abstract published in *Advance ACS Abstracts,* September 1, 1996.

[1] Abbreviations: GAPDH, glyceraldehyde-3-phosphate dehydrogenase; NATA, *N*-acetyltryptophanamide; AMP, adenosine 5′-monophosphate; ADP, adenosine 5′-diphosphate; ADPR, adenosine 5′-diphosphate ribose; RTP, room-temperature phosphorescence; PG, propylene glycol; G3P, glyceraldehyde 3-phosphate; P_i, inorganic phosphate.

S0006-2960(96)00231-0 CCC: $12.00

thermophilus did not reveal any asymmetry in the apo- and holoenzyme (Bieseker & Wonacott, 1977; Skarzynski et al., 1987; Skarzynski & Wonacott, 1988). Moreover, these authors also showed that the tetramer bound to a single NAD^+ molecule is asymmetric and the structure of the ligated subunit is almost identical to that of the holoenzyme, while the structure of the unligated subunits remained very similar to that of the apoenzyme (Leslie & Wonacott, 1984). Such results support ligand-induced sequential conformational changes in GAPDH and are in favor of the induced-fit model.

However, regular crystal-packing forces may influence the conformation of proteins in the crystal state to some extent. In solution, the macromolecule has greater conformational freedom, and for this reason, there is always a concern that the picture portrayed by crystallography is a partial one. For example, there is growing evidence that in solution protein molecules can adopt more than one stable conformation (Frauenfelder et al., 1991; Silva & Weber, 1993; Cioni et al., 1994) possibly endowed with characteristically distinct binding and catalytic properties (Xue & Yeung, 1995). In such cases, conformational equilibria could represent an additional kind of preexisting asymmetry, and if the conformer interconversion is very slow, it would not be easily distinguished from intramolecular asymmetry. As a rule, it is important that crystallographic models of protein structure be confirmed from structural information obtained in dilute solutions. Besides, several studies of NAD^+ binding to GADPH from various origins in solution have been satisfactorily interpreted according to the preexisting asymmetry model assumptions (Seydoux et al., 1973; Branlant et al., 1983; Kelemen et al., 1975; Malhotra et al., 1992).

The present study aims to investigate the solution structure of *B. stearothermophilus* GAPDH and the effects of NAD^+ binding on the conformation of free and bound subunits. Intrinsic fluorescence and phosphorescence emission of its tryptophan (Trp) residues have long been used as monitors of the conformational state of the macromolecule. Spectral energies are sensitive to the polarity of the immediate chromophore's environment, while the excited state lifetimes are indicative of the rate of quenching interactions, such as electron transfer with the nicotinamide moiety of NAD^+ (Vanderkooi et al., 1990), from which distance/orientation relationships may be derived. Finally, the room-temperature phosphorescence (RTP) lifetime (τ_P) provides an exquisite sensitive probe of the local fluidity of the protein matrix (Strambini & Gonnelli, 1985, 1995). This parameter has proven to be a useful tool for uncovering subtle changes in the polypeptide conformation brought about by binding of substrates and allosteric effectors in several enzymes (Cioni & Strambini, 1989; Strambini & Gonnelli, 1990; Strambini et al., 1992), changes otherwise undetected with conventional spectroscopic techniques.

Most GAPDHs of known primary structure possess three Trp residues (W84, W193, and W310), while the enzyme from *B. stearothermophilus* lacks W193. Of course, with multi-tryptophan proteins, the task of relating luminescence data to protein structure is complicated and even impossible if the individual emission properties of each chromophore are not known. A tentative assignment of the individual phosphorescence properties of W310 and W84 was reported for the *B. stearothermophilus* protein (Gabellieri & Strambini, 1989) which, owing to the smaller number of Trp residues, is a simpler system to investigate. Low-temperature phosphorescence studies have shown that the two Trps exhibit distinct phosphorescence spectra, and as a result of differential thermal quenching, only one Trp possesses long-lived RTP (Gabellieri & Strambini, 1989). The long RTP lifetime and its poor O_2 quenching efficiency suggested that RTP originated from a deeply buried Trp, and therefore, the emission was ascribed to W310 in the catalytic domain.

This paper reports the identification of the fluorescence and phosphorescence properties of W310 using a single Trp mutant (W84F) of GAPDH from *B. stearothermophilus*. The luminescence characteristics of W84 are then deduced by difference with the wild-type enzyme. Next, the effects of NAD^+ binding on the extent of fluorescence and phosphorescence quenching by electron transfer to nicotinamide and on the RTP lifetime are examined. Finally, the luminescence of GAPDH at partial degrees of saturation is analyzed for evidence of NAD-induced allosteric transitions in the subunits of the tetramer as might be revealed from a comparison of the emission properties of the apo- and holoenzymes.

MATERIALS AND METHODS

Materials. Charcoal Norit A^R was purchased from Serva (Heidelberg, Germany) and was activated following the procedure described by Henis and Levitzki (1977). *N*-acetyltryptophanamide (NATA) was obtained from Janssen Chimica (Geel, Belgium). Oxidized nicotinamide adenine dinucleotide (NAD^+), adenosine-5′-monophosphate (AMP), and adenosine 5′-diphosphate (ADP) were purchased from Boehringer (Mannheim, Germany); adenosine 5′-diphosphate ribose (ADPR) was from United States Biochemical Co. (Cleveland, OH). All chemicals were of the highest purity grade available from commercial sources and were used without further purification. Doubled distilled MilliQ (Millipore, U.S.A.) water was used throughout.

Site-Directed Mutagenesis, Production, and Purification of Wild-Type and Mutant Enzymes. Construction of recombinant phages and mutagenesis were carried out as previously described by Mougin et al. (1988). Production and purification of wild-type and mutant enzymes were performed in *E. coli* W3CG strain (Ganter & Plückthun, 1990) transformed by the recombinant plasmids. Cells were grown in M63 succinate−glycerol medium, containing ampicillin (100 mg/L) and tetracyclin (15 mg/L). After sonication, GAPDH was purified by ammonium sulfate fractionation and loaded on an ACA 34 gel filtration resin equilibrated in 50 mM Tris buffer and 1 mM EDTA (pH 8.0). Final purification was achieved using a semipreparative Q-Sepharose resin column connected to a FPLC system (Pharmacia). The molecular weight of 35 909 ± 2 determined by mass spectrometry for the W84F mutant was in agreement with the calculated molecular weight of 35 911.

Apoenzymes were prepared by activated charcoal treatment, as described by Henis and Levitzki (1977). Before fluorescence and phosphorescence measurements, the proteins were dialyzed overnight against 20 mM potassium phosphate buffer (pH 7.5) containing 1 mM EDTA. Enzyme concentrations were determined spectrophotometrically, using extinction coefficients (ϵ) at 280 nm of 1.17×10^5 M^{-1} cm^{-1} for apo-WT and 9.42×10^4 M^{-1} cm^{-1} for apo-W84F GAPDH. The molar extinction coefficient of W84F GAPDH

was determined using the method of Gill and von Hippel (1989). Luminescence experiments were carried out at protein concentrations of 3−5 μM, unless otherwise specified.

Enzyme Activity Assay. Enzyme assays were carried out at 25 °C on a Cary 2200 spectrophotometer by monitoring the appearance of NADH at 340 nm. Initial rate measurements for oxidative phosphorylation were performed according to Ferdinand (1964) in 40 mM triethanolamine buffer (pH 8.9) and 0.2 mM EDTA. Apparent Michaelis constants were determined at saturating concentrations of the other substrates or at concentrations chosen to allow maximum rate reaction while avoiding substrate inhibition. The kinetic parameters were deduced from nonlinear regression data analysis.

Fluorescence Measurements. Steady state fluorescence intensity and spectra measurements were performed on a Jasco model FP-770 spectrofluorometer. Fluorescence quantum yields relative to NATA, Φ, were determined in 20 mM potassium phosphate buffer (pH 7.5) using the relationship

$$\frac{\Phi_{\text{prot}}}{\Phi_{\text{NATA}}} = \frac{\int I_{\text{prot}}}{\int I_{\text{NATA}}} \frac{A_{\text{NATA}}}{A_{\text{prot}}}$$

where $\int I$ is the fluorescence intensity integrated over the emission spectrum and A is the absorbance at 295 nm (Parker & Rees, 1960).

Fluorescence intensity decay measurements were performed on a Greg 200 (ISS Inc., Champaign, IL) multifrequency fluorometer, using the cross-correlation phase and modulation method (Gratton et al., 1983). The excitation light (λ_{ex} = 295 nm), provided by a Cermax xenon lamp (LX 300 UV, ILC Technology, Sunnyvale, CA), was modulated by a Pockels cell (frequency range = 10−200 MHz) and selected by a Jobin-Yvon H.10 UV monochromator. The emitted light (λ_{em} >320 nm) was observed through a WG 320 long pass filter to eliminate scattered radiation from the lamp. Phase-shift and demodulation data were fitted in terms of both discrete exponential components and distribution functions (Alcala et al., 1987) using the program Global Analysis (Global Unlimited, LFD, University of Illinois, Urbana). χ^2 values and the spreading of the weighted residuals were used to test the quality of the fitting.

Phosphorescence Measurements. The samples were placed in 4 mm inside diameter cylindrical spectrosil cuvettes. Prior to phosphorescence measurements, oxygen was thoroughly removed from the sample as described by Cioni and Strambini (1989). A conventional homemade instrument was employed for all phosphorescence intensity and spectra measurements (Cioni & Strambini, 1989). Continuous excitation provided by a Cermax xenon lamp (LX 150 UV, ILC Technology) was selected by a 0.25 m grating monochromator (Jobin-Yvon, H25) and the emission dispersed by a 0.25 m grating monochromator (Jobin-Yvon, H25), was detected with an EMI 9635 QB photomultiplier. Phosphorescence decays in fluid room-temperature solutions were measured on an apparatus described before (Strambini & Gonnelli, 1995). Pulsed excitation was provided by a frequency-doubled flash-pumped dye laser (UV 500 M-Candela) (λ_{ex} = 292 nm) with a pulse duration of 1 μs and an energy per pulse of typically 1−10 mJ. The emitted light was collected at 90° from the excitation light and selected by a filter combination with a transmission window between 420 and 480 nm. The photomultipliers were protected from the intense excitation and fluorescence light pulse by a high-speed chopper blade that closed the slits during laser excitation. The minimum dead time of the apparatus was about 10 μs. All the decaying signals were digitized and averaged by a computerscope system (EGAA; RC Electronics). Subsequent analysis of decay curves in terms of discrete exponential components was carried out by a nonlinear least-squares fitting algorithm, implemented by the program Global Analysis. All reported decay data are averages of three or more independent measurements. The reproducibility of τ_P was typically better than 5%.

Table 1: Kinetic Parameters of Wild-Type and Mutant GAPDH[a]

	wild type[b]		mutant	
	K_M (mM)	k_{cat} (s^{-1})	K_M (mM)	k_{cat} (s^{-1})
NAD^+	0.15 ± 0.03		0.11 ± 0.01	
G3P	0.80 ± 0.09	70 ± 6	0.31 ± 0.01	46 ± 1
P_i	8.3 ± 0.6		9.6 ± 0.6	

[a] GAPDH activity was determined at 25 °C in 40 mM triethanolamine buffer (pH 8.9) and 0.2 mM EDTA. The concentrations of the nonvariable substrates were 1 mM G3P, 50 mM P_i, and 1 mM NAD^+. K_M and k_{cat} values are the average of two independent determinations. [b] From Corbier et al. (1994).

RESULTS

Steady State Kinetics. Steady state constants of the mutant and the wild-type enzymes are summarized in Table 1. The K_M values of substrates are not changed to any great extent by the mutation. Moreover, the k_{cat} of the mutant is only reduced by a factor 1.5 compared to that of the wild type. Both observations strongly indicate that the quaternary structure of the protein and the positioning of NAD within the cofactor site are similar in the wild-type and mutant enzymes.

Trp Fluorescence Yields and Decay Kinetics of Trp in W84F Mutant and Wild-Type Apo-GAPDH. The W84F mutant protein possesses a unique Trp residue (W310) which simplifies the characterization of its emission properties. Excitation at 295 nm results in a fluorescence spectrum centered at 330 nm, which is 5 nm red-shifted relative to that of the wild type. The quantum yield relative to NATA, Φ_F, was found to be 0.35 for the mutant and 0.80 for the wild-type protein. If one assumes that the wild-type molar absorptivity at 295 nm is the same for each Trp residue and that no inter-tryptophan energy migration occurs, then the equality $\Phi_F(WT) = [\Phi_F(W84) + \Phi_F(W310)]/2$ yields $\Phi_F(W84) = 1.25$. Thus, the fractional intensities in the wild type are 0.22 for W310 and 0.78 for W84. The assumption that $\Phi_F(W310)$ is the same in both mutant and wild-type proteins requires that the protein environment about the chromophore be unchanged by the mutation and, furthermore, that the two residues in the native enzyme emit independently. While the intra- and intersubunit separation between W84 and W310 is beyond the range of fluorescence energy migration (see Discussion), the identity of the phosphorescence spectrum of W310 in mutant and wild-type proteins (see below) suggests that its environment is unchanged by the mutation.

The fluorescence decay characteristics (λ_{em} > 320 nm, see Figure 1) were determined by the phase and modulation

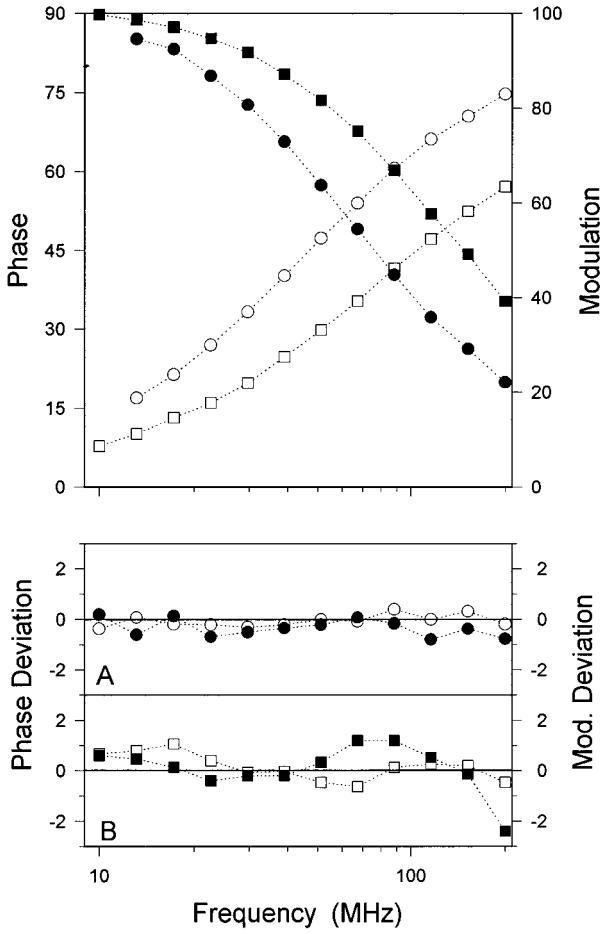

FIGURE 1: Frequency response of Trp fluorescence ($\lambda_{ex} = 295$ nm, $\lambda_{em} \geq 320$ nm) from native (○, ●) and mutant (□, ■) apo-GAPDH in phosphate buffer (20 mM, pH 7.5) at 20 °C. The experimental phase and modulation were fitted to a biexponential law, and the phase (○, □) and modulation (●, ■) deviations are shown in the bottom panel: (A) native protein and (B) mutant protein.

Table 2: Trp Fluorescence Parameters of Wild-Type and W84F GAPDH Derived from Fitting the Frequency Response in Terms of Discrete Lifetime Components

protein	Trp residue	Φ_F (relative to NATA)	τ_1 (ns)	τ_2 (ns)	α_1	χ^2
W84F mutant	310	0.35	0.77	2.59	0.61	6.5
wild type	310 + 84	0.80	1.93	4.24	0.39	1.6
wild type− W84F mutant	84	1.25[a]	3.25[a]	5.6[a]	0.66[a]	0.96

[a] Values estimated from fitting wild-type data assuming the emission from W310 to be independent and identical to that in the W84F mutant (see text).

method. Figure 1 compares the frequency response of mutant and wild-type GAPDH. The frequency response of the mutant relative to that of the wild type is shifted to higher frequencies. In both cases, the magnitude of χ^2 and the asymmetry in the residue distribution indicate that at least two lifetime components are required to fit the data. Data analysis in terms of two discrete components is reported in Table 2. The mutant protein exhibits a shorter-lived fluorescence, and the preexponential terms (α_i) indicate that about 60% of the intensity decays with a lifetime (τ_i) of 0.77 ns. This value is small relative to the typical 3−5 ns lifetime of unperturbed Trp in proteins and implies that the emission of W310 is substantially quenched. It is evident from the

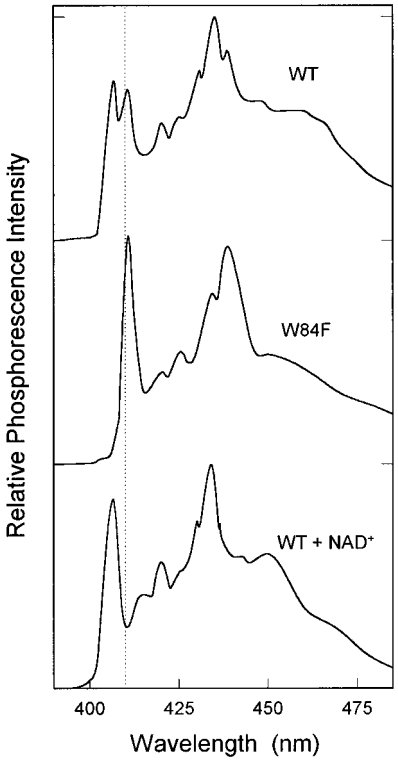

FIGURE 2: Trp phosphorescence spectra ($\lambda_{ex} = 295$ nm) of apo- and holo-GAPDH (wild type) and apo-GAPDH mutant in PG/buffer (50/50, w/w) glass at 140 K. The protein concentration was typically 10^{-5} M (subunits), and that of NAD^+ was 10^{-4} M.

frequency response of the wild-type protein that the fluorescence decay of W84 is slower and falls within expected values. An approximate estimate of its decay parameters, α_i and τ_i, may be derived by fitting the frequency response of the wild type in terms of independent contributions of the two Trp residues, assuming again that the emission in W310 has the same characteristics as in the mutant. Data analysis carried out by taking the fractional intensity of W310 to be 0.22 and maintaining invariant its values of α_i and τ_i yielded an adequate fit only if two additional lifetime components of 3.25 and 5.6 ns, with relative weights of 0.66 and 0.34, respectively, were included (Table 2).

Trp Phosphorescence of W84F Mutant and Wild-Type Apo-GAPDH in Low-Temperature Glasses. The phosphorescence spectra ($\lambda_{ex} = 295$ nm) of mutant and wild-type GAPDH in PG/buffer (50/50, w/w) glasses at 140 K are compared in Figure 2. As previously reported (Gabellieri & Strambini, 1989), the wild-type spectrum shows an evident splitting of the 0,0 vibronic band into two components centred at 406.5 and 410.5 nm, the distinct spectral energies reflecting the different nature of the chromophores' environment. The mutant spectrum exhibits a single 0,0 vibronic band that peaked at the same wavelength of the red 0,0 vibronic band in the wild-type spectrum. Hence, the 410.5 nm band of the wild type must be assigned to W310 and, by exclusion, the 406.5 nm band to W84.

The phosphorescence decay kinetics of W310 in the mutant protein, obtained with steady state excitation to minimize the short-lived ($\tau \approx 0.8$ s) contribution from the organic cosolvent (typically less than 5%), is not exponential. Analyzed in terms of two discrete exponential components, it yielded lifetimes of 2.6 s (relative weight $\alpha = 0.41$) and 5.7 s ($\alpha = 0.59$). In glass matrices, lifetimes smaller than

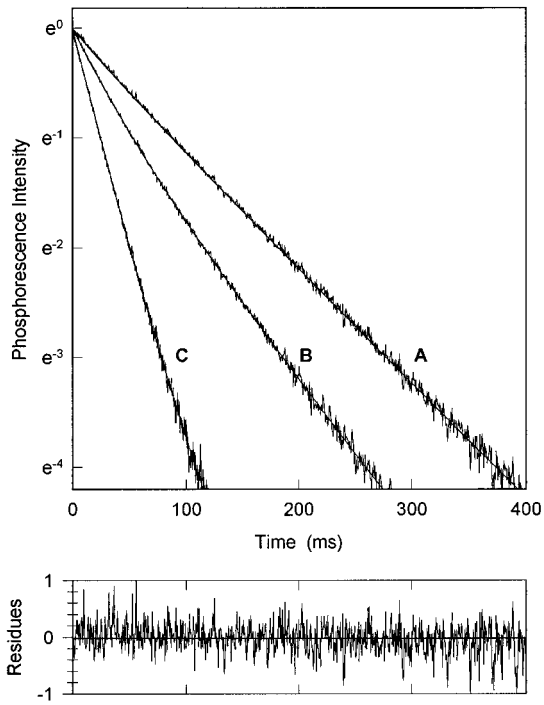

FIGURE 3: Examples of phosphorescence decays (λ_{ex} = 295 nm, 420 nm < λ_{em} < 480 nm) of native GAPDH in phosphate buffer at 20 °C: (A) apoprotein, (B) GAPDH bound to two NAD^+ molecules, and (C) holoprotein ([NAD^+] = 10^{-4} M). Protein concentration as in Figure 2. The distribution of residues refers to a fitting of the apoprotein decay with three exponential components.

5 s are unusual and so far have been reported only for Trp residues that are in proximity of disulfide bridges or perturbed by prosthetic groups. As neither of these situations applies to the environment of W310, we must conclude that the small lifetime in 40% of the subunits is due to an as yet unidentified perturbation by some neighboring amino acid side chains. The decay kinetics of W84 in the wild-type protein can be determined selectively without interference from W310 since the latter does not contribute to the emission at wavelengths shorter than 408 nm. The phosphorescence intensity at 406 nm, corrected for the solvent emission, decays essentially in an exponential fashion with a lifetime of 6.7 s.

Trp Room-Temperature Phosphorescence (RTP) of Mutant and Wild-Type Apo-GAPDH. The phosphorescence of W310 (the 410.5 nm band), in mutant and wild-type proteins alike, is drastically quenched in fluid solutions. In buffer (20 mM phosphate and 1 mM EDTA at pH 7.5) at 20 °C, the mutant RTP decay is adequately described by a single exponential with a lifetime of 0.05 ms. This value of τ is over 20-fold smaller compared to the lifetime of free Trp in solution and implies that τ_{W310} is dominated by a strong quenching interaction (Gonnelli & Strambini, 1995). Interestingly, at room temperature, the decay is homogeneous which indicates that the distinct W310-quencher configurations inferred from the nonexponential decay in glasses are in rapid equilibrium on the microsecond time scale.

The phosphorescence decay of the wild-type protein in buffer, at 20 °C, is much slower and highly nonexponential (Figure 3). The emission is dominated by a component with a lifetime τ_1 of 96 ms (α_2 = 0.73) with the remainder displaying two shorter lifetimes, τ_2 = 43 ms (α_2 = 0.15) and τ_3 = 0.05 ms (α_3 = 0.12). τ_3 is so similar to τ_{W310} of the mutant protein that the rapidly decaying component should be ascribed to W310. This analysis leads to the conclusion that the decay of W84 is moderately heterogeneous, implying that in about 17% of the subunits τ_{W84} is less than $^1/_2$ of the value exhibited in the rest. The amplitude of the 43 ms component was found to vary between 0.15 and 0.04 from one apopreparation to another. Such variability suggests that the sample is not wholly apo- or native-like. Completely NAD^+ free preparations are not readily obtained, and the charcoal treatment, with extensive adsorption of GAPDH on the solid surface, is likely to partly damage the native structure. We point out that the short-lived components were not resolved in the previous study of GAPDH phosphorescence (Gabellieri & Strambini, 1989), and the reasons are to be found in the large dead time of the apparatus together with excitation by a continuous, less intense, light source.

Quenching of Trp Fluorescence by NAD^+. In phosphate buffer (20 mM phosphate and 1 mM EDTA at pH 7.5), at 20 °C, NAD^+ quenches Trp fluorescence by 55 ± 2% in the mutant and 35 ± 1% in the wild-type protein. Titration experiments showed that ligand binding to the high-affinity first and second sites results in 25 and 50% quenching, respectively, an indication that the extent of fluorescence quenching is proportional to the degree of saturation. Relative to W310, W84 is less severely quenched by NAD^+. The intensity drop of W84 fluorescence can be estimated from a comparison of the residual fluorescence intensities of the mutant and wild-type holoproteins (0.45 and 0.65, respectively), assuming that W310 is quenched to the same extent in both macromolecules. Considering that W310 contributes to 22% of the total wild-type fluorescence, the equation $(F_{holo}/F_{apo})_{WT} = 0.78(F_{holo}/F_{apo})_{W84} + 0.22(F_{holo}/F_{apo})_{W310}$ yields $(F_{holo}/F_{apo})_{W84} = 0.71$, which means that roughly 30% of the W84 fluorescence is quenched by NAD^+.

The frequency response of the mutant protein fluorescence was determined at degrees of saturation of 0.25, 0.50, and 1.0. The results are shown in Figure 4 (for the wild type, the pattern is very similar, although, as might be expected, the overall change is smaller). Binding of NAD^+ results in a progressive shift of the phase/modulation curves to higher frequencies, indicating a continuous decrease in fluorescence lifetime. At complete NAD^+ saturation, the mutant holoprotein data are adequately described in terms of discrete components with lifetimes of 0.44 ns (α = 0.87) and 3.05 ns (α = 0.13) [the decrease in average lifetime ($\tau_{av} = \tau_1\alpha_1 + \tau_2\alpha_2$) from apo to holo forms (53%) is commensurate with the drop in fluorescence intensity (55%), and this excludes additional contributions from static quenching]. Partially saturated forms require at least three lifetime components to yield satisfactory fitting statistics, but the procedure does not recover lifetime values that are related to those of apo or holo forms. To test whether this finding necessarily implies peculiar W310 decay kinetics at partial saturation, the data were also fitted with fixed parameters (α and τ) representing apo and holo forms appropriately weighted for their expected contribution to the overall intensity. Good values of χ^2 (χ^2 = 3 and 2.8, respectively, for 0.25 and 0.5 saturation degrees) and symmetric distributions of residues do also indicate that this model provides an appropriate description of the fluorescence decay at intermediate NAD^+ saturation.

Continuous distributions of lifetime components were also used as an alternative approach to the analysis of nonexpo-

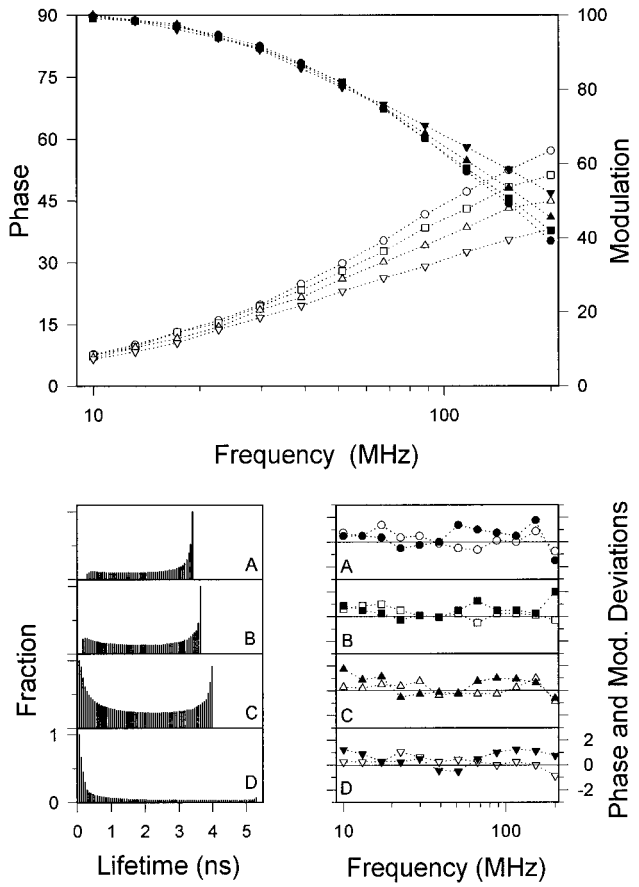

FIGURE 4: (Upper panel) Effects of NAD^+ binding on the frequency response of W310 fluorescence in the mutant protein: apoprotein (○, ●), 25% NAD^+ saturation (□, ■), 50% NAD^+ saturation (△, ▲), and holoprotein (▽, ▼). (Lower left panel) Asymmetric Planck's distribution functions, $f(\tau) = N\tau^{-1}\{\ln[\tau(\tau_H-\tau_L)/\tau_H(\tau-\tau_L)]\}^{\beta}$ (Alcala et al., 1987), obtained from fitting the data above: A = apoprotein ($\beta = -0.478$), B = 25% saturation ($\beta = -0.417$), C = 50% saturation ($\beta = -0.39$), and D = holoprotein ($\beta = -0.196$). (Lower right panel) Corresponding phase (empty symbols) and modulation (full symbols) deviations. Experimental conditions are as in Figure 1.

nential decays. For any set of phase/modulation data, a single Gaussian or Lorentzian distribution function failed to provide an adequate fit of the frequency response. Satisfactory fits were obtained with an asymmetric Planck's distribution function (Alcala et al., 1987). As shown in Figure 4b, the lifetime distributions are asymmetric for both apo- and holoproteins, with the former and latter weighted in favor of large and small lifetime values, respectively. At partial saturation, the lifetime distribution functions are intermediate between these two extremes and are again approximately described by a linear combination of apo and holo distribution functions, as if the decay of empty and filled subunits remained invariant with the degree of saturation. Planck's distributions describe heterogeneous decays arising from chromophores frozen into distinct environments, unable to exchange during the excited state lifetime. The frequency response of the mutant fluorescence is thus consistent with a multitude of W310 quenching configurations, static on the nanosecond time scale, that are affected by NAD^+ binding in a way which is by and large independent of the degree of saturation.

The native protein fluorescence is intrinsically more complex and the perturbation introduced by NAD^+ binding is substantially smaller than in the mutant protein. For these reasons, an analysis of the frequency response in terms of specific models is not warranted.

Effects of NAD^+ Binding on the Low-Temperature Phosphorescence. In PG/buffer glasses, at 140 K, the phosphorescence of W310 in both mutant and wild-type proteins is totally quenched by a NAD^+. At a mutant protein concentration of 10 μM (subunits) and a NAD^+ concentration between 10^{-5} and 10^{-4} M, the residual phosphorescence intensity is 2−3%, which is less than the solvent emission (≈5%). This small Trp component has a lifetime similar to that of the apoprotein and presumably represents a small fraction of subunits unable to bind NAD^+. At partial NAD^+ saturation (0.25 and 0.5), the residual phosphorescence intensity of the mutant protein was found to be directly proportional to the degree of saturation. Importantly, its spectral characteristics and decay kinetics remained undistinguishable from those of the apoprotein. Thus, as with fluorescence, these results imply that NAD^+ quenches W310 emission exclusively in the ligated subunits. Furthermore, the invariance of the phosphorescence spectrum at partial saturation shows that, in glasses, any possible conformational change associated with NAD^+ complexation does not influence the emission of W310 in the empty subunits.

The phosphorescence spectrum of NAD^+-saturated wild-type GAPDH is shown in Figure 2. Unlike the W84 band at 406.5 nm, the emission of W310 at 410.5 nm is totally quenched. The intensity of the 406.5 nm band is 30 ± 2% lower than in the apoprotein, the reduction being commensurate with the estimated quenching of W84 fluorescence (29%). Its lifetime is essentially constant at all degrees of saturation tested, which is consistent with the lack of any influence of NAD^+ on the triplet state of W84.

Influence of NAD^+ Binding on the RTP Lifetime of W310 and W84. In contrast to that in low-temperature glasses, the short-lived RTP emission of W310 in the mutant protein is not significantly affected by NAD^+ binding. In phosphate buffer, at 20 °C, the decay is always monoexponential and the lifetime is constant at 50 ± 5 μs for any degree of saturation ($[NAD^+] \leq 10^{-4}$ M). Thus, the electron-exchange interaction between NAD^+ and W310, which effectively quenches the long-lived phosphorescence in glasses, does not seem to compete with the rapid internal quenching process responsible for the short RTP lifetime.

The effect of NAD^+ on the RTP decay of W84 in the wild-type protein can be studied selectively as its RTP lifetime is roughly 1000-fold greater than that of W310. At a NAD^+ concentration (40 μM) which corresponds to a degree of saturation of 0.95, the phosphorescence decay of W84 is essentially monoexponential with a lifetime τ_{holo} 33 ± 1 ms. The decay is clearly heterogeneous at intermediate saturation (Figure 3), but the fitting procedure yielded two constant lifetimes throughout. The values of τ_i and α_i are displayed in Figure 5 as a function of ν, the number of NAD^+ molecules bound per tetramer. When $\nu \geq 1$, as ν increases, a greater fraction of the intensity decays with a roughly constant lifetime of 34 ± 3 ms, almost identical to τ_{holo}. The remaining emission, presumably originating from NAD^+ free subunits, exhibits a constant lifetime of about 80 ms, a value distinctly smaller than that of 95 ms of the apoprotein.

Figure 5 also reports the expected amplitudes of the 80 and 33 ms lifetime components (when $\nu \geq 1$) if these were to be associated to free and NAD^+-bound subunits, respectively. In the theoretical estimate of the amplitudes, account

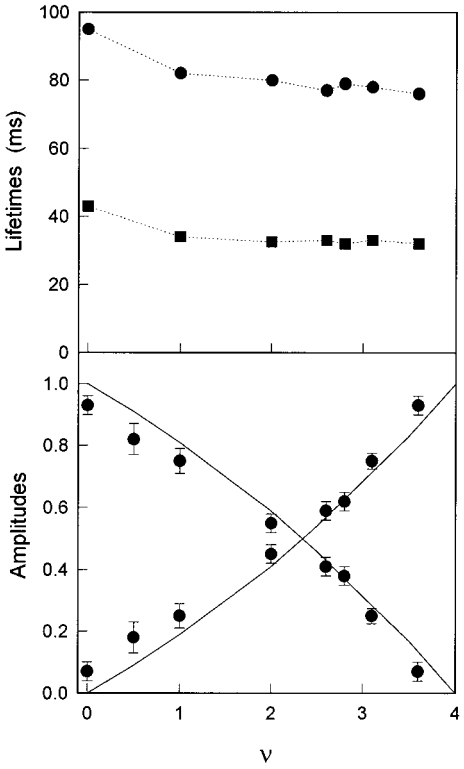

FIGURE 5: RTP lifetimes and amplitudes of W84 as a function of ν, the number of NAD^+ molecules bound per tetramer, derived from a biexponential fitting of phosphorescence decays. The reported values are the average of three separate determinations, and the standard deviations of the amplitudes are indicated with error bars. Conditions are as in Figure 3. Full lines represent theoretical amplitudes expected if ligated and unligated subunits possessed constant lifetimes of 33 and 80 ms, respectively.

was taken of the reduced (30% less) phosphorescence yield of W84 in NAD^+-bound subunits. In the lower ν range, the theoretical prediction yields a 10−15% smaller amplitude for the 33 ms component but the agreement with experimental data improves at larger ν values. Considering that in the apoprotein decay about 15% of the intensity exhibits a lifetime of about 40 ms, not readily distinguishable from τ_{holo}, the agreement between this model and experiment is quite satisfactory. Thus, binding of NAD^+ to one or more subunits of the tetramer reduces the RTP lifetime of W84 in both filled and empty subunits, the former acquiring a value of τ similar to that of the holoprotein. It should be mentioned that if NAD^+ binding and release occurred appreciably during the phosphorescence decay its effect would be to lower τ_{apo} and raise τ_{holo} of empty and filled subunits, respectively, the lifetime averaging process becoming more important at larger degrees of saturation (i.e. on occupation of lower-affinity sites). The invariance of τ_{holo} and τ_{apo} throughout the saturation curve suggests that NAD^+ exchange is slow on the phosphorescence time scale.

Influence of NAD^+ Analogues on the RTP of W84. Binding of AMP, ADP, and ADPR to GAPDH does not affect the Trp luminescence except for modest variations in the RTP lifetime of W84. Table 3 reports the lifetimes and corresponding amplitudes obtained from fitting the phosphorescence decay (neglecting the small microsecond component, see above) in terms of two discrete components, together with the ligand concentrations employed. In each case, τ_{W84} is reduced, the effect being pronounced only with ADPR.

Table 3: Influence of NAD^+ Analogues on the RTP Lifetime of W84

sample	[ligand] (mM)	K^a (M)	$\tau_1{}^b$ (ms)	$\tau_2{}^b$ (ms)	$\alpha_1{}^b$
apo-wild type	−	−	96	43	0.85
wild type + AMP	10	3.8×10^{-5}	80	34	0.79
wild type + ADP	5	4.4×10^{-5}	70	28	0.78
wild type + ADPR	0.47	4.5×10^{-5}	51	29	0.84

[a] Henis and Levitzki (1980). [b] Reproducibility of the fitting data is about 5%.

DISCUSSION

Fluorescence and Phosphorescence Characteristics of W310 and W84 in Apo-GAPDH. The construction of a GAPDH mutant lacking W84 has permitted the identification of the individual fluorescence and phosphorescence characteristics of the two Trp residues in the native *B. stearothermophilus* enzyme. The deduction process involved two assumptions: (1) the fluorescence emission of W310 is not affected by the mutation and (2) the two aromatic residues emit independently of each other so that the properties of W84 could be derived from the difference between the mutant and wild-type protein luminescence. The first assumption is supported by the fact that the mutation did not alter the phosphorescence spectrum or the RTP lifetime of W310. Because both parameters depend critically on the chromophore's environment, we conclude that the protein structure surrounding W310 and consequently its fluorescence are unchanged by the mutation. The second assumption is also reasonable, since the two Trp residues of GAPDH are effectively located far from each other, the minimum intra- and intersubunit distance between W310 and W84 (R_{min} = 2.2 nm) being larger than the critical distance R_o of ≤ 1.3 nm (Willaert et al., 1992) for efficient fluorescence energy migration. Furthermore, the orientation of the transition dipole moments (L_a states) between the closest pair of Trps (W84 and W310 in the same subunit) is unfavorable for energy transfer.

The fluorescence emission of W310 is intrinsically quenched and contributes to only about 22% of the total fluorescence of the native enzyme. Its spectrum is 5−6 nm red-shifted relative to that of W84, and its decay kinetics are rapid (with subnanosecond lifetimes) and heterogeneous. While the short lifetime indicates that the excited singlet state of W310 is perturbed by a quenching moiety in its proximity, the heterogeneous decay suggests that multiple chromophore−quenchers configurations are resolvable in the nanosecond time window. The fluorescence of W84, by contrast, is intense, and its slightly heterogeneous decay with lifetimes of 3−5 ns is typical of unperturbed Trp residues in proteins. Interestingly, this finding excludes that nearby His 108 is a quencher of Trp 84 fluorescence as previously postulated for the rabbit and porcine GAPDHs (Davis & Maki, 1984).

The 0,0 vibronic band of the phosphorescence spectrum of W310 in the mutant protein is centered at 410.5 nm, the same wavelength as the red 0,0 band in the composite spectrum of the native protein. This spectral identity assigns unequivocally the 410.5 nm band to W310 and the 406.5 nm band to W84. Thanks to spectral resolution, the decay kinetics of W84 in the wild-type protein could be studied selectively at 406 nm without interference from W310. W84

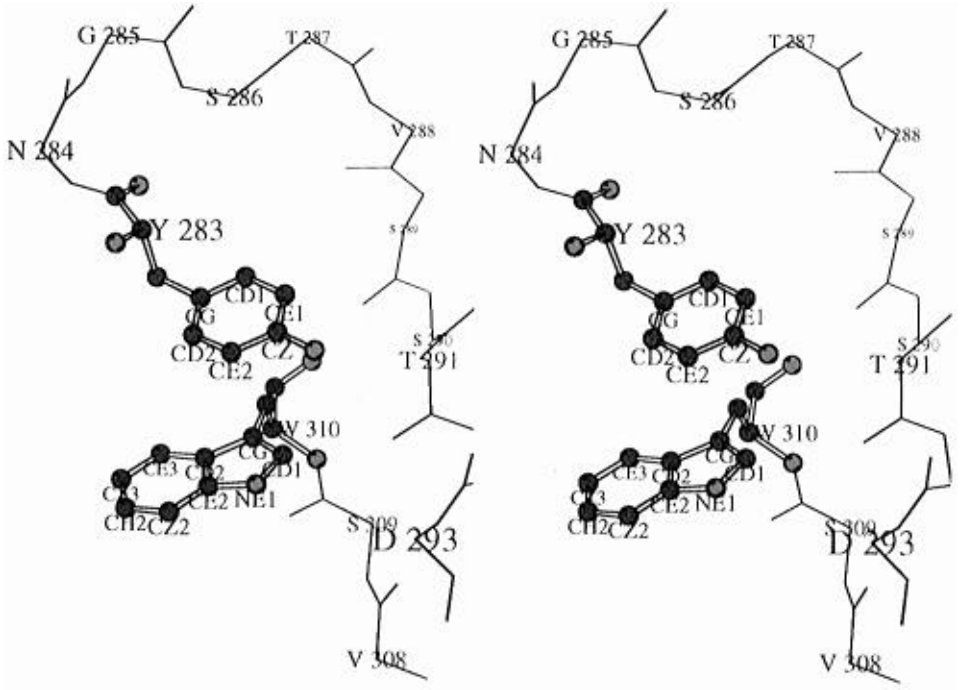

FIGURE 6: Position of Tyr 283 relative to Trp 310 (apostructure). The angle between the planes through the aromatic rings is 11° 36′.

exhibits a typical phosphorescence lifetime (~6 s) in glasses and a relatively long-lived RTP lifetime (~100 ms) that attests to a considerable local peptide rigidity. In contrast, the phosphorescence of W310, as is its fluorescence, is clearly perturbed and heterogeneous. In rigid glasses, τ_{W310} is smaller than the 5−7 s lifetime of Trp in proteins or free in solution. The difference is even larger at ambient temperature, where τ_{W310} is 10-fold smaller than τ of Trp free in solution. Clearly, τ_{W310} is dominated by a local quenching, and because of it, it no longer represents a probe of protein flexibility (Strambini & Gonnelli, 1995). Interestingly, the heterogeneity in the phosphorescence decay of W310 is observed in rigid glasses but not in room-temperature solutions. This implies that, while distinct quencher−W310 configurations are frozen out in glasses, at ambient temperature they interconvert rapidly during the ~50 μs triplet lifetime. Should the same quenching group also be responsible for the short fluorescence lifetime of W310, then its multiple fluorescence lifetimes at ambient temperature demonstrate that the above structural fluctuations, rapid in the microsecond time window, are slow on the microsecond time scale. In order to identify the putative quenching side chain(s), we recall that the quencher amino acid must lie in close proximity (0.2−0.3 nm) to the indole ring (Strambini & Gonnelli, 1995). The side chains that are located within a 0.6 nm shell (atom edge to atom edge) about the aromatic ring of W310 are Asp, Arg, Thr, Ser, Pro, Val, Leu, Ile, and Tyr. Of these, only Tyr is an effective quencher of Trp phosphorescence (Gonnelli & Strambini, 1995), and thus, we propose that the perturbation of W310 phosphorescence and fluorescence originates from the stacking interaction between the Trp indole and the phenol ring of Y283 (see Figure 6). Replacing Tyr 283 with Val or Ile, residues which are present at position 283 in certain GAPDH sequences, could confirm this hypothesis.

It must be mentioned that the present identification of the phosphorescence properties of W310 and W84 contradicts the previous tentative assignment of phosphorescence bands (Gabellieri & Strambini, 1989). The main criterion adopted in that assignment was the phosphorescence thermal-quenching profile, i.e., the progressive decrease of τ as the temperature is raised from the glass state to ambient temperature. The rationale was that τ is a monitor of the local fluidity of the protein matrix and the largest decrease in τ is therefore expected for Trp residues located in flexible protein environments. Because peripheral regions of the protein globule (site of W84) are generally more flexible than well-structured inner cores (site of W310), it seemed reasonable to attribute the thermally quenched 410.5 nm band to W84 and the long-lived RTP to W310. Misleading in this conclusion was the unsuspected phosphorescence-quenching potential of neutral Tyr, only recently discovered (Gonnelli & Strambini, 1995). By the same criterion were assigned the three-component spectra (including W193) of muscle (pig and rabbit) and yeast GAPDH (Davis & Maki, 1984; Strambini & Gabellieri, 1989), assignments that, in the light of the present findings, need to be reexamined. In all these proteins, only one residue exhibits long-lived RTP. With the muscle enzymes, its spectrum is identical to that of the bacterial protein, and therefore, it is plausible that the same residue (W84) is involved. Another striking similarity with W84 of *B. stearothermophilus* GAPDH is that its phosphorescence is not quenched by NAD^+ binding (E. Gabellieri and G. B. Strambini, unpublished observations), implying that this Trp residue must reside outside the range of the nicotinamide interaction. The crystallographic structure of the lobster GAPDH (Buehner et al., 1974), *B. stearothermophilus* GAPDH (Skarzynski et al., 1987), and *E. coli* GAPDH (Duee et al., 1996) does confirm that W84 is located far from the nicotinamide moiety.

Effects of NAD^+ Binding on Trp Luminescence. NAD^+ complexation affects GAPDH fluorescence and phosphorescence in two ways: (1) it introduces a quenching interaction between indole and the nicotinamide moiety and (2) it induces changes in the subunit conformation that alter the dynamical structure of the chromophore's environment.

For each Trp, both the fluorescence yield and the lifetime decrease substantially upon NAD^+ binding. Their individual decay kinetics remain heterogeneous also in the holoprotein, from which we infer multiple quenching rates and therefore multiple Trp−NAD^+ configurations. The long-range quenching reaction must involve an electron-transfer step (Vanderkooi et al., 1990) as the emission/absorption spectral overlap integral for energy transfer is negligibly small. Marcus's theory (Marcus & Sutin, 1985) predicts an exponential dependence of the electron-transfer rate on the donor−acceptor distance, and therefore, knowledge of the distance dependence of the process, i.e., the preexponential factor and the attenuation length, allows a prediction to be made as to whether the quenching reaction between Trp and NAD^+ is exclusively intrasubunit. An average transfer rate $\langle k_{et}\rangle$ may be estimated from the average lifetime in the apoprotein, $\langle\tau_0\rangle = \sum\alpha_i\tau_i$, and the decrease in fluorescence yield, Φ/Φ_0:

$$\langle k_{et}\rangle = 1/\langle\tau_0\rangle(\Phi/\Phi_0 - 1)$$

where it is implicitly assumed that fluorescence quenching is entirely due to electron transfer to nicotinamide (support for this assumption comes from the complexes with coenzyme analogues lacking the nicotinamide ring). For W310, the center−center distance between indole and nicotinamide rings, r_{W310}, is 1.78 nm and $\langle k_{et}\rangle_{W310} = 8.2 \times 10^8\ s^{-1}$. W84 is farther removed ($r_{W84} = 1.95$ nm) and as expected is characterized by a smaller rate ($\langle k_{et}\rangle_{W84} = 10^8\ s^{-1}$). A similar value ($\langle k_{et}\rangle = 4 \times 10^8\ s^{-1}$) was derived for the electron-transfer process between NAD^+ and W314 of liver alcohol dehydrogenase (Strambini & Gonnelli, 1990), where $r_{W314} = 1.75$ nm. With these data, an estimate of the distance dependence of the rate, assuming the upper bound value of $10^{13}\ s^{-1}$ for the contact transfer rate (Marcus & Sutin, 1985), yields $k_{et}(r) = 10^{13}\exp[-8.1(r\text{-}r_0)]$, where r is the distance in nanometers and r_0 is the distance of closest approach. This law, although approximate, predicts that the electron-transfer rate between NAD^+ and the nearest Trp of the other subunits ($r = 2.5$ nm) is negligibly small ($2.0 \times 10^6\ s^{-1}$) relative to the fluorescence decay rate ($1/\tau > 2 \times 10^8\ s^{-1}$) and confirms that quenching is exclusively intrasubunit. This conclusion is important because variations in the extent of quenching along the NAD^+ saturation profile would necessarily imply nonequivalent NAD^+−Trp geometrical arrangements.

Electron exchange with the excited-triplet state is much slower and markedly different between W310 and W84. At low temperatures, the phosphorescence of W310 is totally quenched by NAD^+ whereas the emission of W84 is unaffected. Considering the long triplet lifetimes in glasses and the precision of these measurements, we infer that $k_{et}(W310) \geq 2\ s^{-1}$ and $k_{et}(W84) \leq 0.02\ s^{-1}$. An upper bound for $k_{et}(W310)$ is $10^3\ s^{-1}$ since τ_{W310} at 20 °C is constant at 50 μs with and without NAD^+. This large, over 100-fold, difference between $k_{et}(W310)$ and $k_{et}(W84)$ is not accounted for by the typical distance dependence of electron-transfer processes and probably reveals an unusually large donor−acceptor orientation effect.

Changes in the dynamical structure of the Trp environment as a result of the coenzyme-induced polypeptide rearrangements are promptly revealed by the RTP lifetime. In this respect, the only effect of NAD^+ binding to GAPDH is a 3-fold reduction of τ_{W84}, a change which attests to an increased flexibility of the holostructure in the coenzyme binding domain. Significantly, X-ray crystallographic data show appreciable holo−apo structural differences in the region of W84 but not in the catalytic domain hosting W310 (Skarzynski & Wonacott, 1988). Also consistent with X-ray data is the finding that the decay of W84 in the holoprotein is homogeneous, implying that the τ-averaged structure of the subunits in the fully bound tetramer is equivalent.

Binding of NAD^+ analogues devoid of the nicotinamide moiety (AMP, ADP, and ADP ribose) does not alter the Trp luminescence characteristics of GAPDH except for the RTP lifetime of W84. Their effect is, as with NAD^+, to reduce τ_{W84}, the change being modest with AMP and ADP but rather pronounced with ADPR. These results point out that both the adenine nucleotide moiety and the ribose ring play a role in modifying the apostructure toward a conformation intermediate between apo and holo forms. Again, these findings are fully consistent with crystallographic studies that report minor conformational changes of the apostructure ligated with AMP or ADP (Biesecker & Wonacott, 1977) but infer larger transitions with ADP ribose which, like NAD^+ and NADH, causes cracking of the apoenzyme crystals.

Trp Luminescence and Structural Heterogeneity of GAPDH Subunits at Partial Degrees of NAD^+ Saturation. The sharp dependence of the electron-transfer rate on the distance/orientation between indole and nicotinamide rings and the sensitivity of the RTP lifetime on the flexibility of the polypeptide structure represent two important monitors of the subunit conformation. The former is useful for distinguishing different coenzyme−Trp configurations in the ligated subunit, the latter for reporting differences in the conformation of the coenzyme binding domain (W84) of empty and filled subunits at partial NAD^+ saturation, relative to the apo- and holostructure, respectively. The picture that emerges from our results at partial saturation suggests that the Trp−NAD^+ configuration and the conformational state of ligated subunits is holo-like, whereas the structure of the empty subunits is not wholly apo-like. Indeed, the extent of fluorescence quenching by NAD^+ at partial saturation, in both mutant and wild-type proteins, reveals a constant quenching efficiency in each subunit of the tetramer and thus plausibly a similar if not unique Trps−nicotinamide geometrical arrangement. Analysis of the fluorescence decay of W310 in the mutant protein at intermediate saturation also shows that between one and three NAD^+ molecules bound per tetramer the lifetime distribution is compatible with a superimposition of apo and holo lifetime distributions in the appropriate ratio. Furthermore, the RTP lifetime of W84 drops to about $^1/_3$ of its initial value (95 to 33 ms) as a result of the coenzyme-induced conformational change. At intermediate NAD^+ saturation, the decay of W84 RTP reveals two constant lifetime components throughout, ligated subunits exhibiting a lifetime of 34 ms, identical to the holoprotein, and NAD^+ free subunits a lifetime of 80 ms. Since the latter is significantly smaller than the 95 ms lifetime of the apoprotein, the triplet probe provides evidence of coenzyme-induced conformational changes also in the empty subunits. It may be argued that the difference in τ_{W84} between the apoprotein and the empty subunits of partially saturated tetramers is modest and therefore does not reveal extensive conformational changes. However, it must be pointed out that W84 lies at the periphery of the globular unit, removed from the subunit interface across which the

conformational change is transmitted. Larger rearrangements could occur at the active site pocket which is not far from the subunit interface. Our conclusion is in agreement with the crystal structure of 1-NAD GAPDH published by Leslie and Wonacott (1984) which indicated a holo-like structure for the ligated subunit and smaller adjustments in the structure of the empty subunits.

In summary, the experimental findings reported here allow a number of conclusions to be drawn about the intrinsic luminescence of GAPDH and on the subunit structure of the protein in the apo and holo forms, some of which are definitely shown by the data, others which are inferred by it. Among the former we list the following.

(1) First is the correct assignment of the individual phosphorescence characteristics of W84 and W310 as well as the demonstration that W310 is selectively quenched by NAD^+.

(2) Next is the demonstration that both fluorescence and phosphorescence quenching, in both WT and mutant proteins, are proportional to the degree of NAD^+ saturation. Since the Trp−NAD^+ interaction is strictly intrasubunit and is critically dependent on the distance/orientation between chromophores, this finding implies an equivalence in Trp−NAD^+ arrangement in filled subunits at all degrees of saturation.

(3) Last is the demonstration that the NAD^+−induced apo to holo transition produces an increased flexibility of the polypeptide about W84. Importantly, since the amplitude of τ_{W84} (holo) is proportional to the fraction of NAD^+-bound subunits, it must be concluded that the apo−holo structural change is sequential.

Other deductions are more indirect or are subject to the validity of one or more assumptions. Among these are the following.

(1) First is the knowledge of the individual fluorescence characteristics of W84 and W310 in apo- and holo-GAPDH, as it is assumed that no energy migration occurs between chromophores and that the emission of W310 is the same in mutant and wild-type proteins.

(2) Next is the fully symmetric state and structural equivalence of the subunits in apo- and holotetramers as deduced from RTP τ_{W84}. For the apo sample, the assumption is that the small and variable fraction of intensity with a smaller lifetime represents a nonnative apo form. For the holoprotein, the assumption is that the rate of coenzyme exchange between free and bound states is slow on the phosphorescence time scale so as not to average out an otherwise heterogeneous decay.

(3) Last is the NAD^+-induced structural change in empty subunits at a partial degree of saturation from the decrease in τ_{W84}. Again, the assumption is that lifetime averaging by NAD^+ exchange is negligible.

Overall, the present spectroscopic investigation of the solution structure of GAPDH and its NAD^+-induced conformational changes by and large confirms the picture portrayed by crystallographic studies. The complete apo−holo transition requires the nicotinamide moiety, although the ADPR part of the coenzyme by itself elicits a substantial rearrangement of the apostructure in the direction of a holo-like structure. Most importantly, the data suggest that the NAD^+-induced conformational change is sequential and that NAD^+ binding could result in a rearrangement of the structure of the empty subunits. Since the holostructure of the subunits seems to be invariant at intermediate degrees of saturation, it is plausible that the structural bases for the decreased coenzyme affinity, i.e., negative cooperativity, are to be found in the rearrangement of the empty subunits. Taken altogether, this set of evidence strongly suggests that NAD^+ binds to GAPDH according to an induced-fit model.

ACKNOWLEDGMENT

The authors are grateful to Prof. E. Gratton for his advice with fluorescence lifetime measurements. The technical assistance of A. Puntoni and Dr. C. Corbier and the help of Mrs. C. Neri in preparing the manuscript are duely acknowledged. We are also very indebted to Drs. Potier and Van Dorsselaer for performing the mass spectrum analysis of the proteins and to Dr. G. Mulliert-Carlin for the Figure.

REFERENCES

Alcala, R., Gratton, E., & Prendergast, F. G. (1987) *Biophys. J. 51*, 925−936.
Allen, G., & Harris, J. I. (1975) *Biochem. J. 151*, 747−749.
Bieseker, G., & Wonacott, A. J. (1977) *Biochem. Soc. Trans. 5*, 649−654.
Branlant, G., & Branlant, C. (1985) *Eur. J. Biochem. 150*, 61−66.
Branlant, G., Eiler, B., Biellmann, J. F., Lutz, H. P., & Luisi, H. P. (1983) *Biochemistry 22*, 4437−4443.
Buehner, M., Ford, G. G., Moras, D., Olsen, K. W., & Rossman, M. G. (1974) *J. Mol. Biol. 82*, 563−585.
Cioni, P., & Strambini, G. B. (1989) *J. Mol. Biol. 207*, 237−247.
Cioni, P., & Strambini, G. B. (1994) *J. Mol. Biol. 242*, 291−301.
Cioni, P., Gabellieri, E., Gonnelli, M., & Strambini, G. B. (1994) *Biophys. Chem. 52*, 25−34.
Clermont, S., Corbier, C., Mely, Y., Gerard, D., Wonacott, A., & Branlant, G. (1993) *Biochemistry 32*, 10178−10184.
Conway, A., & Koshland, D. E., Jr. (1968) *Biochemistry 7*, 4011−4022.
Corbier, C., Mougin, A., Mely, Y., Adolph, H. W., Zeppezauer, M., Gerard, D., Wonacott, A., & Branlant, G. (1990) *Biochimie 72*, 545−554.
Corbier, C., Michels, S., Wonacott, A. J., & Branlant, G. (1994) *Biochemistry 33*, 3260−3265.
Davis, J. M., & Maki, A. H. (1984) *Biochemistry 23*, 6249−6256.
Duee, E., Olivier-Deyris, L., Fanchon, E., Corbier, C., Branlant, G., & Dideberg, O. (1996) *J. Mol. Biol. 257*, 814−838.
Ferdinand, W. (1964) *Biochem. J. 92*, 578−585.
Frauenfelder, H., Sligar, S. G., & Wolyner, P. G. (1991) *Science 254*, 1598−1602.
Gabellieri, E., & Strambini, G. B. (1989) *Biophys. Chem. 33*, 257−264.
Ganter, C., & Plückthun, A. (1990) *Biochemistry 29*, 9395−9402.
Gill, Y. I., & von Hippel, P. H. (1989) *Anal. Biochem. 182*, 319−326.
Gonnelli, M., & Strambini, G. B. (1995) *Biochemistry 34*, 13847−13857.
Gratton, E., Jameson, D. M., Rosato, N., & Weber, G. (1983) *Rev. Sci. Instrum. 55*, 488−494.
Harris, J. I., & Waters, M. (1976) in *The Enzymes 13* (Boyer, P. D., Ed.) 3rd ed., pp 1−49, Academic Press, Inc., New York.
Henis, Y. I., & Levitzki, A. (1977) *J. Mol. Biol. 117*, 699−716.
Henis, Y. I., & Levitzki, A. (1980) *Eur. J. Biochem. 112*, 59−73.
Kelemen, N., Kellershohn, N., & Seydoux, F. (1975) *Eur. J. Biochem. 57*, 69−78.
Koshland, D. E., Jr., Nemethy, G., & Filmer, D. (1966) *Biochemistry 5*, 365−385.
Leslie, A. G. W., & Wonacott, A. J. (1984) *J. Mol. Biol. 178*, 743−772.
Malhotra, O. P., & Bernhardt, S. A. (1968) *J. Biol. Chem. 243*, 1243−1252.
Malhotra, O. P., Tikoo, K., Kayastha, A. M., Srinivasan, T. R., & Gupta, A. K. (1992) *Indian J. Biochem. Biophys. 29*, 469−476.
Marcus, R. A., & Sutin, N. (1985) *Biochim. Biophys. Acta 811*, 265−322.

Moras, D., Olsen, K., Sabesan, M. N., Buehner, M., Ford, G. G., & Rossman, M. G. (1975) *J. Biol. Chem. 250*, 9137−9162.
Mougin, A., Corbier, C., Soukri, A., Wonacott, A., Branlant, C., & Branlant, G. (1988) *Protein Eng. 2*, 45−48
Parker, C. A., & Rees, W. T. (1960) *Analyst 85*, 587−600.
Seydoux, F., Bernhardt, S., Pfenninger, O., Payne, M., & Malhotra, O. P. (1973) *Biochemistry 12*, 4290−4300.
Seydoux, F., Malhotra, O. P., & Bernhardt, S. A. (1974) *CRC Crit. Rev. Biochem. 2*, 227−257.
Silva, J. L., & Weber, G. (1993) *Annu. Rev. Phys. Chem. 44*, 89−113.
Skarzynski, T., & Wonacott, A. J. (1988) *J. Mol. Biol. 203*, 1097−1118.
Skarzynski, T., Moody, P.-C. E., & Wonacott, A. J. (1987) *J. Mol. Biol. 193*, 171−187.
Strambini, G. B., & Gonnelli, M. (1985) *Chem. Phys. Lett. 115*, 196−200.
Strambini, G. B., & Gonnelli, M. (1990) *Biochemistry 29*, 196−203.
Strambini, G. B., & Gonnelli, M. (1995) *J. Am. Chem. Soc. 117*, 7646−7651.
Strambini, G. B., Cioni, P., Peracchi, A., & Mozzarelli, A. (1992) *Biochemistry 31*, 7535−7542.
Trentham, D. R. (1968) *Biochem. J. 109*, 603−612.
Vanderkooi, J. M., Calhoun, D. B., & Englander, S. W. (1987) *Science 236*, 568−569.
Vanderkooi, J. M., Englander, S. W., Papp, S., Wright, W. W., & Owen, C. S. (1990) *Proc. Natl. Acad. Sci. U.S.A. 87*, 5099−5103.
Willaert, K., Loewenthal, R., Sancho, J., Froeyen, M., Fersht, A., & Engelborghs, Y. (1992) *Biochemistry 31*, 711−716.
Xue, Q., & Yeung, E. (1995) *Science 373*, 681−683.

BI960231B